Inelastic cotunneling mediated singlet-triplet transition in carbon nanotubes

S. Moriyama,[1,*] J. Martinek,[2,3] G. Ilnicki,[2] T. Fuse,[1] and K. Ishibashi[1]
[1]*Advanced Device Laboratory, RIKEN, 2-1, Hirosawa, Wako, Saitama 351-0198, Japan*
[2]*Institute of Molecular Physics, Polish Academy of Sciences, 60-179 Poznań, Poland*
[3]*Institute for Materials Research, Tohoku University, Sendai 980-77, Japan*
(Received 19 May 2009; published 17 July 2009)

We investigate electronic transport through single-wall carbon-nanotube quantum dots weakly coupled to metallic leads in the Coulomb-blockade regime. While sequential tunneling is suppressed, the transport, due to correlated tunneling of two electrons cotunneling, is possible. We report on a pronounced current peak for the singlet-triplet transition mediated by inelastic cotunneling processes that allows for their separation from the elastic components. Using the second-order perturbation theory in the tunnel-coupling strength we are able to fit it into the experimental data, explain the details of the line shape, and extract values of parameters that describe pseudospin asymmetry.

DOI: 10.1103/PhysRevB.80.033408 PACS number(s): 73.63.Fg, 73.22.−f, 73.23.Hk

Single-walled carbon nanotubes (SWNTs) are one of the attractive materials for one-dimensional electronic systems[1] and furthermore, quantum dots (QDs) can be formed in an individual SWNT with weak coupling contacts to electrodes.[2–7] Transport mechanism through a QD is determined by the Coulomb-blockade (CB) effect.[8] However, higher-order tunneling events dominate the transport at low temperature. A second-order tunneling process, cotunneling, is the simplest many-body phenomenon since only two electrons are involved.[9–12] It is possible to calculate it exactly using the second-order perturbation theory[13,14] also in the nonequilibrium regime that makes it a very good test of the theory.

A "closed" metallic SWNT QD shows four-electron shell structures that originate from both the twofold spin degeneracy and the predicted twofold subband degeneracy due to the SWNT's unique band structures.[4–7] Magnetic fields can induce the singlet-triplet (ST) transition mediated by the two closed orbitals at half-shell filling. The evidence of the ST transition in QDs has been observed in the higher-order tunneling events in transport measurements with strong-coupling regime, where the Kondo effect appears simultaneously[15–21] but second-order perturbation theory is insufficient to explain observed experimental data. In this Brief Report, we study ST transition in the cotunneling regime using an experimental approach by detecting the inelastic cotunneling resonance in the current in response to a magnetic field. We demonstrate that our technique allows for: (i) separation of the elastic and inelastic cotunneling components, (ii) precise fitting to the second-order perturbation theory (the extraction of various information about the effective pseudospin asymmetries), and (iii) determines the presence of spin-flip relaxation. The experimental results are in excellent agreement with the theory indicating that the effective pseudospin asymmetry is presented in a single SWNT QD and strong spin-flip relaxation occurs in a half-shell filling regime.

Our sample is comprised of an individual SWNT contacted by evaporating Ti (40 nm) for source and drain electrodes on a SiO_2/Si substrate. The distance between the contacts was designed to be 300 nm. The whole nanotube between the contacts behaved as a single quantum dot at low temperature.[6,22] All measurements were performed in a dilution refrigerator and a magnetic field was applied perpendicular to the tube axis.

The model Hamiltonian for a carbon-nanotube quantum dot with two highest occupied orbital levels, $m=A,B$, and spin σ at energies $\epsilon_{m\sigma}$ coupled to metallic leads is given by

$$H=\sum_{rk\sigma}\varepsilon_{rk\sigma}c^{\dagger}_{rk\sigma}c_{rk\sigma}+\epsilon_{m\sigma}\sum_{m\sigma}d^{\dagger}_{m\sigma}d_{m\sigma}+\frac{U}{2}\left(n-\frac{1}{2}\right)^2+\sum_{rkm\sigma}(V_{rkm}d^{\dagger}_{m\sigma}c_{rk\sigma}+V^{*}_{rkm}c^{\dagger}_{rk\sigma}d_{m\sigma}), \quad (1)$$

where $c_{rk\sigma}$ and $d_{m\sigma}$ are the Fermi operators for electrons in the leads, $r=L,R$, and in the QD. Here, V_{rkm} denotes the tunneling amplitude, $n=\Sigma_{m\sigma}d^{\dagger}_{m\sigma}d_{m\sigma}$ is dot's occupation. The difference $\epsilon_{m\uparrow}-\epsilon_{m\downarrow}=\Delta_Z=g\mu_B B$ is induced by a magnetic field. The orbital degeneracy is lifted by amount $\delta=\epsilon_{B\sigma}-\epsilon_{A\sigma}$. We discuss the cotunneling transport in the CB valleys in which dot's occupancy is fixed. Considering two levels we take into account quantum fluctuations between the four states $\alpha=|A\uparrow\rangle,|A\downarrow\rangle,|B\uparrow\rangle,|B\downarrow\rangle$. The tunnel-coupling strength is characterized by $\Gamma^{\alpha}_{r}=2\pi\rho_{r\sigma}|V_{rm}|^2$, where $\rho_{r\sigma}$ denotes density of states (for simplicity, we ignore k dependence of $V_{rmk}=V_{rm}$). For nonmagnetic leads we consider that there is no spin asymmetry $\rho_{r\uparrow}=\rho_{r\downarrow}$, however, there is possible asymmetry in orbital coupling $V_{rA}\neq V_{rB}$, which we model by two parameters, P_P and P_A, $\Gamma^{A,B\sigma}_{L}=(1\pm P_A)(1\mp P_P)\Gamma$ and $\Gamma^{A,B\sigma}_{R}=\Gamma(1\mp P_A)(1\mp P_P)\Gamma$. Here, the upper (lower) signs refer to orbital A (B) so that P_P (P for parallel) describes asymmetry in coupling of orbitals A and B to the leads. In other words, when P_P increases, the coupling of orbital A (B) to the leads decreases (increases). Analogically, P_A (A for antiparallel) describes asymmetry in coupling that is exactly opposite for both leads (a sign change in front of P_A). It means that if P_A increases, the coupling of orbital A to the lead L (R) increases (decreases) while the coupling of orbital B to lead L (R) decreases (increases) by the same ratio. Using the second-order perturbation theory we determine the rate $\gamma^{\alpha,\beta}_{rr'}$ for a cotunneling process in which one electron leaves the dot to the reservoir r' and another electron enters from r with the initial and final dot state being α and β, respectively. For $\alpha\neq\beta$, i.e., inelastic cotunneling, the rate is given by

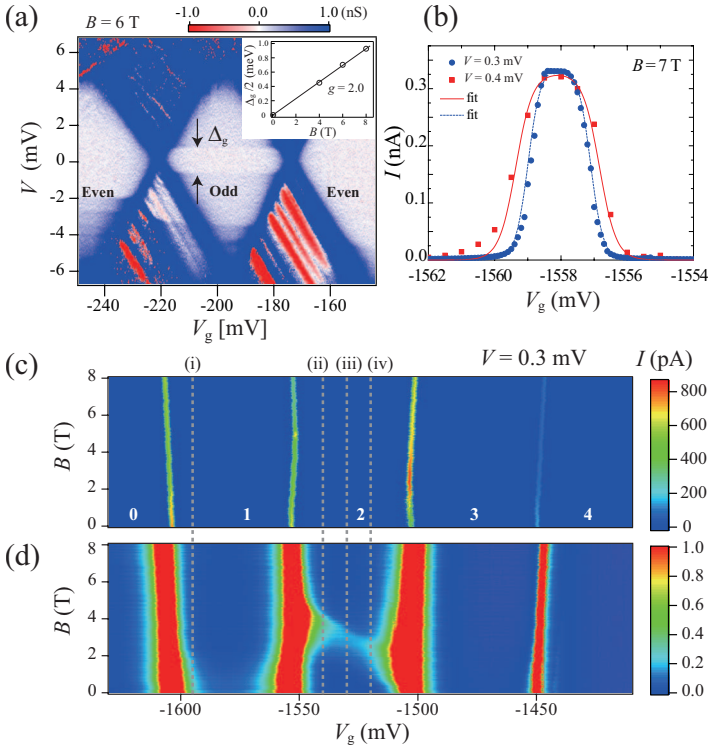

FIG. 1. (Color) (a) Differential conductance dI/dV as a function of V and V_g at $B=6$ T and $T_e=120$ mK. Inelastic cotunneling gap (Δ_g) due to the Zeeman effect of a single-particle level is indicated by arrows. Inset: magnetic field dependence of Δ_g. (b) Fitting of a typical Coulomb peak. (c) Magnetic field evolution of the Coulomb peaks measured with $V=0.3$ mV in a four-electron shell, where n indicates the number of electrons in a shell at $T_e=240$ mK. (d) Same data as (c) but different current range to show the cotunneling features mediated the spin 1/2 and the ST transition.

$$\gamma_{rr'}^{\alpha,\beta} = \frac{\Gamma_r^\alpha \Gamma_{r'}^\beta}{h} P \int d\omega d\omega' f(\omega)[1-f(\omega')][1/(\omega'+\mu_{r'}-\epsilon_\alpha) + 1/(\epsilon_\beta+U-\omega-\mu_r)]^2 \delta(\omega+\mu_r-\omega'+\mu_{r'}+\epsilon_\alpha-\epsilon_\beta), \tag{2}$$

where $f(\omega)$ denotes the Fermi function, μ_r is the electrochemical potential, and P denotes the principal value of integral.[23] For $\alpha=\beta$, when the dot state is not changed, i.e., for elastic cotunneling, we get

$$\gamma_{rr'}^{\alpha} = \frac{1}{h} P \int d\omega d\omega' f(\omega)[1-f(\omega')]\delta(\omega+\mu_r-\omega'+\mu_{r'}) \times \left[\frac{\Gamma_r^\alpha \Gamma_{r'}^\alpha}{(\omega'+\mu_{r'}-\epsilon_\alpha)^2} + \frac{\Gamma_r^{\bar{\alpha}} \Gamma_{r'}^{\bar{\alpha}}}{(\epsilon_{\bar{\alpha}}+U-\omega-\mu_r)^2} \right]. \tag{3}$$

The current $I=I_{\rm el}+I_{\rm inel}$ can be separated into the elastic, $I_{\rm el}$, and inelastic, $I_{\rm inel}$, component

$$I_{\rm el} = e\sum_\alpha p_\alpha(\gamma_{\rm LR}^\alpha - \gamma_{\rm RL}^\alpha), \quad I_{\rm inel} = e\sum_{\alpha\neq\beta} p_\alpha(\gamma_{\rm LR}^{\alpha\beta} - \gamma_{\rm RL}^{\alpha\beta}), \tag{4}$$

where p_α is the probability of occupation of state α.

We investigate two regimes: (i) when there is a single, $n=1$, and (ii) two electrons, $n=2$, on the dot. Since in our experiment $\delta \gg k_B T, eV$, then (i) for $n=1$ the orbital B is empty so probabilities $p_{B\uparrow}=p_{B\downarrow}=0$ and $p_{A\uparrow}$ with $p_{A\downarrow}$ are determined below. (ii) For $n=2$, where also two states are possible, the orbital A can be either doubly occupied and then it forms a singlet state, $|S\rangle=d_{A\uparrow}^\dagger d_{A\downarrow}^\dagger|0\rangle$, while the orbital B is empty or together with orbital B is singly occupied that forms a triplet state, $|T+\rangle=d_{A\uparrow}^\dagger d_{B\uparrow}^\dagger|0\rangle$ considering $\Delta_Z \geq 0$. Probabilities $p_{B\downarrow}=0$ and $p_{A\uparrow}=1$, and probabilities $p_{A\uparrow}=p_{|S\rangle}$ and $p_{B\downarrow}=p_{|T+\rangle}$ are determined below. For both cases the undetermined probabilities p_α and p_β are obtained from stationary rate equation $0=\Sigma_{rr'}(p_\alpha \gamma_{rr'}^{\alpha\beta} - p_\beta \gamma_{rr'}^{\beta\alpha})$ together with the normalization condition $p_\alpha+p_\beta=1$.

In the weak-coupling regime, when the current is weak, the intradot spin flip and orbital-orbital relaxation become relevant. In this regime, the level occupation of the dot approaches the Boltzman distribution that can be obtained from the generalized rate equation $0=p_\alpha R(\epsilon_\alpha-\epsilon_\beta)-p_\beta R(\epsilon_\beta-\epsilon_\alpha)+\Sigma_{rr'}(p_\alpha \gamma_{rr'}^{\alpha\beta}-p_\beta \gamma_{rr'}^{\beta\alpha})$, where the relaxation rate is given by $R(\omega)=R_{\rm sf}\exp(-\omega/2k_BT)$.

Figure 1(a) shows a plot of the differential conductance $dI/dV(V,V_g)$ as a function of the bias voltage V and the gate V_g at $B=6$ T in even-odd regime. A typical cotunneling gap is observed in the Coulomb diamond of odd number of electrons, that is, independent of gate voltage.[9–12] The inset of Fig. 1(a) shows the magnetic field dependence of the gap width that is linear and indicates that the g factor, $g\approx 2.0$.

In order to study the ST transition in the cotunneling regime, we proceed to investigate the four-electron shell structure. The magnetic field evolution of each Coulomb peak for one shell for the same sample on a different cooldown at $T_e=240$ mK is shown in Figs. 1(c) and 1(d). The current presented in Fig. 1(c) is due to sequential tunneling transport and the presence of the ST transition can be deduced by the change in the line slopes.[6,7] In Fig. 1(b), there is a cross section of the sequential tunneling line with expected rectangular shape and thermal smearing. By changing the current range by three orders of magnitude one obtains Fig. 1(d), where lines from Fig. 1(c) become much broader demonstrating transport due to the cotunneling. In addition to the broadening some additional signal appears close to $B=0$ and $n=1,3$, as well as for half filling ($n=2$) and $B>0$ where the

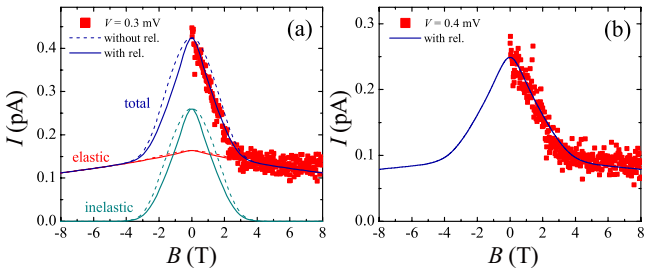

FIG. 2. (Color online) Cotunneling current taken from the valley with a single occupancy ($n=1$) in Fig. 1(d) indicated by the horizontal dashed line (i). Solid (dotted) line is a theory plot for inelastic, elastic, and total cotunneling current for $S=1/2$ at the dot, (a) $V=0.3$ mV, (b) $V=0.4$ mV, and in the presence (absence) of strong spin-flip relaxation.

new line connects the two kinks at the $1\leftrightarrow 2$ and $2\leftrightarrow 3$ sequential tunneling lines.

We study in detail the line shape of the additional signal starting with $n=1$. Figure 2 shows the theoretical fitting of the cotunneling current taken from valley with one electron in Fig. 1(d) indicated by the vertical dotted line (i), $V_g=-1.595$ V. Using Eqs. (2)–(4), we model the transport where the only fitting parameters are constant background and overall current amplitude, which can be estimated using value of $\Gamma\approx 0.015$ meV (obtained for the sequential regime). In Fig. 2(a) one can distinguish the inelastic components that exist only for $eV>\Delta_Z$ and the elastic ones weakly depending on B which serve as a background for the inelastic component. For a weak spin-flip relaxation, $R_{sf}\ll\Gamma$, theory predicts a parabolic dependence for $\Delta_Z/eV\ll 1$ that can be obtained analytically. Deep inside the CB regime, where we neglect corrections in the ratios X/Y with $Y=|\epsilon|,\epsilon+U$ and $X=k_BT$, and keep the lowest-order corrections for $X=eV$ we find

$$I_{\rm inel}=G_0\Gamma^2(1-P_{\rm P}^2)\left[\frac{1}{|\epsilon|}+\frac{1}{\epsilon+U}\right]^2\left[1-2\left(\frac{\Delta}{eV}\right)^2\right]V, \quad (5)$$

$$I_{\rm el}=G_0\Gamma^2\left[\frac{1}{\epsilon^2}+\frac{1}{(\epsilon+U)^2}\right]V-2\left[\frac{1}{|\epsilon|^3}+\frac{1}{(\epsilon+U)^3}\right]\frac{\Delta^2}{e}, \quad (6)$$

where $G_0=e^2/h$, $\Delta=\Delta_Z$, $\epsilon=(\epsilon_{A\uparrow}+\epsilon_{A\downarrow})/2$, and for nonmagnetic leads $P_P=P_A=0$. There is a clear discrepancy between theory (dashed line) and experimental results in Fig. 2(a). Note that the linewidth is not a fitting parameter since it is extracted from the experiment via the ratio Δ/eV. Therefore, it is necessary to study the opposite limit $R_{sf}\gg\Gamma$ and then theory predicts a linear dependence on Δ given by

$$I_{\rm inel}=G_0\Gamma^2(1-P_{\rm P}^2)[1/|\epsilon|+1/(\epsilon+U)]^2[V-\Delta/e], \quad (7)$$

$$I_{\rm el}=G_0\Gamma^2(1-P_{\rm A}^2)V\{[1/\epsilon^2+1/(\epsilon+U)^2]-[1/|\epsilon|^3+1/(\epsilon+U)^3]\Delta\}, \quad (8)$$

that is, in good agreement with the experiment indicating that a strong spin-flip relaxation occurs in the QD.

Using Eqs. (2)–(4), we can also model the cotunneling current for the ST transition, however, situation becomes

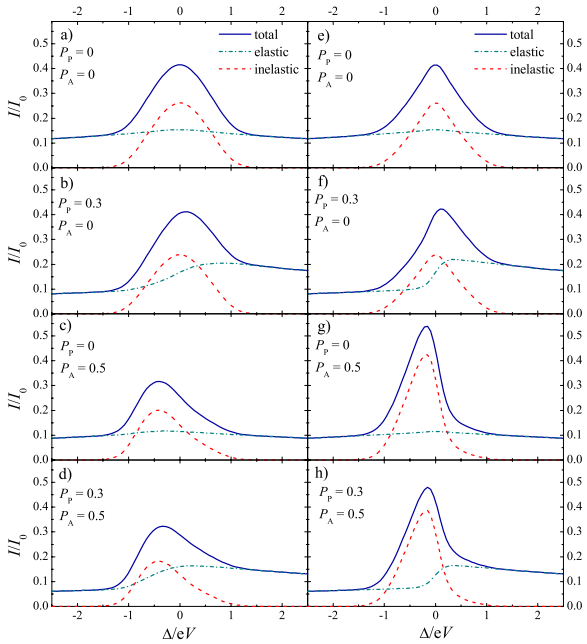

FIG. 3. (Color online) Calculated cotunneling line shape as a function of the tuned magnetic field from the resonance condition for various pseudospin asymmetries. The contribution from the elastic (dotted-dashed line) and the inelastic cotunneling (dashed line) is depicted. Plots (a)–(d) are with long and (e)–(h) with short spin-flip relaxation time; (a) and (e) for a full symmetry $P_P=0$ and $P_A=0$; (b) and (f) $P_P=0.3$ and (c) and (g) $P_A=-0.5$; (d) and (h) both asymmetries are present: $P_P=0.3$ and $P_A=-0.5$. Other parameters are $k_BT/eV=0.1$, $\epsilon/eV=-7.8$, $U/eV=-26.7$ (extracted from Fig. 1), and $I_0=e\Gamma_L\Gamma_R/(2\pi\hbar U)$.

more complex since the asymmetry in the coupling is possible, $P_P\neq 0$ and $P_A\neq 0$. One can interpret the asymmetry parameters as an effective pseudospin polarization since both orbitals possess the opposite spin indices. Figure 3 shows the calculated cotunneling line shape as a function of the tuned magnetic field, Δ, from the resonance condition for various pseudospin asymmetries, where left (right) panel is for weak, $R_{sf}\ll\Gamma$, (strong, $R_{sf}\gg\Gamma$) spin-flip relaxation. Again, we can describe the experimental results using formulas given by Eqs. (5)–(8), where now $\Delta=\epsilon_{B\downarrow}-\epsilon_{A\uparrow}$ and $\epsilon=(\epsilon_{B\downarrow}+\epsilon_{A\uparrow})/2$. Equations (5)–(7) are valid only for $P_A=0$ and Eqs. (6) and (7) for $P_P=0$. The lack of asymmetry, Figs. 3(a) and 3(e), has already been discussed above. In the presence of the asymmetry in coupling of both orbitals, $P_P\neq 0$ but keeping $P_A=0$ [Figs. 3(b) and 3(f)] the inelastic cotunneling line does not change the shape [Eqs. (5) and (7), respectively] since both orbitals participate in each inelastic process. Only its amplitude is reduced by $(1-P_P^2)$. For the elastic transport, there is formation of the step, since depending on the sign of Δ, only one of the orbitals is strongly populated while only one of them is strongly coupled to the electrodes. It leads to enhancement of transport by $(1+P_P)^2$ and reduction by $(1-P_P)^2$ for opposite sides providing asymmetric line shape.

For antisymmetric coupling of orbitals, $P_A\neq 0$ and $P_P=0$, there is symmetry for elastic processes that amplitude is only reduced by $(1-P_A^2)$ and strong asymmetry in coupling for inelastic transport that leads to additional spin accumula-

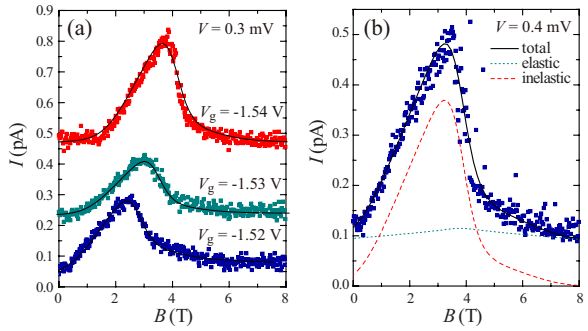

FIG. 4. (Color online) (a) Cotunneling current (with artificial offset) for the singlet-triplet transition taken form Fig. 1(d) at half-shell filling ($n=2$) for $V=0.3$ mV, indicated by horizontal dashed lines (ii)–(iv), respectively. The theory lines are plotted in the strong relaxation limit for the spin asymmetry $P_A=0.5$ and $P_P=0.0$, 0.2, and 0.3, respectively. (b) The cotunneling current for $V=0.4$ mV while $P_A=0.45$ and $P_P=0.0$.

tion and strong asymmetry in inelastic line shape depending on the sign of Δ [Figs. 3(c) and 3(g)]. A strong increase in the amplitude of the inelastic component in the presence of the strong spin-flip relaxation, $R_{sf} \gg \Gamma$, proves the role of the spin accumulation that suppresses the transport in the opposite limit, $R_{sf} \ll \Gamma$ (the spin blockade). For strong relaxation, $R_{sf} \gg \Gamma$ ratio for the transport between the positive and negative values of Δ is on the order of $[(1-P_A)/(1+P_A)]^2$ leading to pronounced asymmetry and shift of the total maximum away from $\Delta=0$. When both $P_P \neq 0$ and $P_A \neq 0$ [Figs. 3(d) and 3(h)] we have superposition effects discussed above. Figure 4 shows the theoretical fitting of the cotunneling current at half-shell filling ($n=2$) in Fig. 1(d), indicated by the vertical dotted lines. Good agreement with the theory allows for the extraction of values of the asymmetry parameters P_P and P_A.

The coupling of both orbitals to the leads can be different, which leads to effective spin asymmetry. Both orbitals have different spin indices. Then, this situation is similar to a dot coupled to ferromagnetic leads,[14] where the spin asymmetry appears in the natural way due to spin-dependent density of states. The pseudospin asymmetries, P_P and P_A can be interpreted as effective spin polarization for the ferromagnetic leads with parallel and antiparallel alignments, respectively. There were several effects and applications predicted for QDs coupled to ferromagnetic leads that can be realized now in this geometry. In Fig. 4(a), we demonstrate that the value of the effective spin polarization can be modified and controlled by the gate voltage by means of the electric field that can be important for the effective spin control and manipulation at the dot. We should also expect steps in dI/dV for $n=2$ but dI/dV at half-shell filling is extremely noisy so it was difficult to observe any gap that demonstrates the power of our approach. Our results indicate that strong spin-flip relaxation occurs in a QD with $\tau_{sf}<0.3$ μs (estimated form the cotunneling current magnitude) and provide information about the effective pseudospin asymmetry.

In summary, we have carried out the cotunneling transport measurements in SWNT QDs and investigated the ST transition using inelastic cotunneling current. Using the second-order perturbation theory we have succeeded to get excellent agreement with the experimental results, explained the complex shape of transport characteristics, and demonstrated the presence of the strong pseudospin asymmetry in a dot.

We thank J. Barnaś, J. König, S. Maekawa, Yu. V. Nazarov, Y. Utsumi, I. Weymann, and G. Schön for helpful discussions. This work was supported in part by the Grant-in-Aid for Young Scientists (A) under Grant No. 20686008 from the MEXT of Japan, the Polish grant for science in years 2006–2009 as a research project, and the CAS at the Norwegian Academy of Science and Letters.

*Present address: National Institute for Materials Science, 1-1, Namiki, Tsukuba, Ibaraki 305-0044, Japan.

[1] R. Saito *et al.*, *Physical Properties of Carbon Nanotubes* (Imperial College, London, 1998).
[2] D. H. Cobden *et al.*, Phys. Rev. Lett. **81**, 681 (1998).
[3] S. J. Tans *et al.*, Nature (London) **394**, 761 (1998).
[4] W. Liang, M. Bockrath, and H. Park, Phys. Rev. Lett. **88**, 126801 (2002).
[5] D. H. Cobden and J. Nygård, Phys. Rev. Lett. **89**, 046803 (2002).
[6] S. Moriyama *et al.*, Phys. Rev. Lett. **94**, 186806 (2005).
[7] A. Makarovski *et al.*, Phys. Rev. B **74**, 155431 (2006).
[8] H. Grabert and M. H. Devoret, *Single Charge Tunneling* (Plenum, New York, London, 1991), Chap. 5; *Mesoscopic Electron Transport*, edited by L. L. Sohn, L. P. Kouwenhoven, and G. Schön (Kluwer, Dordrecht, 1997).
[9] S. De Franceschi *et al.*, Phys. Rev. Lett. **86**, 878 (2001).
[10] D. M. Zumbühl *et al.*, Phys. Rev. Lett. **93**, 256801 (2004).
[11] A. Kogan *et al.*, Phys. Rev. Lett. **93**, 166602 (2004).
[12] R. Schleser *et al.*, Phys. Rev. Lett. **94**, 206805 (2005).
[13] D. V. Averin and A. A. Odintsov, Phys. Lett. A **140**, 251 (1989); D. V. Averin and Yu. V. Nazarov, Phys. Rev. Lett. **65**, 2446 (1990); K. Kang and B. I. Min, Phys. Rev. B **55**, 15412 (1997).
[14] I. Weymann, J. Barnas, J. Konig, J. Martinek, and G. Schon, Phys. Rev. B **72**, 113301 (2005); I. Weymann, J. Konig, J. Martinek, J. Barnas, and G. Schon, *ibid.* **72**, 115334 (2005).
[15] S. Sasaki *et al.*, Nature (London) **405**, 764 (2000).
[16] J. Nygård *et al.*, Nature (London) **408**, 342 (2000).
[17] A. Kogan, G. Granger, M. A. Kastner, D. Goldhaber-Gordon, and H. Shtrikman, Phys. Rev. B **67**, 113309 (2003).
[18] B. Babić, T. Kontos, and C. Schonenberger, Phys. Rev. B **70**, 235419 (2004).
[19] P. Jarillo-Herrero *et al.*, Nature (London) **434**, 484 (2005).
[20] P. Jarillo-Herrero, J. Kong, H. S. J. van der Zant, C. Dekker, L. P. Kouwenhoven, and S. De Franceschi, Phys. Rev. Lett. **94**, 156802 (2005).
[21] J. Paaske *et al.*, Nat. Phys. **2**, 460 (2006).
[22] S. Moriyama, T. Fuse, T. Yamaguchi, and K. Ishibashi, Phys. Rev. B **76**, 045102 (2007).
[23] J. König, J. Schmid, H. Schoeller, and G. Schön, Phys. Rev. B **54**, 16820 (1996).